



Examination of the lung and lymphoid tissue mRNA transcriptome response in dairy calves following experimental challenge with bovine alphaherpesvirus one (BoHV-1)

Title	Examination of the lung and lymphoid tissue mRNA transcriptome response in dairy calves following experimental challenge with bovine alphaherpesvirus one (BoHV-1)
Author(s)	O'Donoghue, Stephanie; Earley, Bernadette; Johnston, Dayle; Finnie, Matthew S.; Cosby, S. Louise; Lemon, Ken; McMenamy, Michael J.; Taylor, Jeremy F.; Kim, Jae Woo; Morris, Derek W.; Waters, Sinéad M.
Publication Date	2025-05-02
Publisher	Public Library of Science
Repository DOI	https://doi.org/10.1371/journal.pone.0319575

RESEARCH ARTICLE

Examination of the lung and lymphoid tissue mRNA transcriptome response in dairy calves following experimental challenge with bovine alphaherpesvirus one (BoHV-1)

Stephanie O'Donoghue^{1,2}, Bernadette Earley¹, Dayle Johnston¹, Matthew S. Finnie¹, S. Louise Cosby³, Ken Lemon³, Michael J. McMenemy³, Jeremy F. Taylor⁴, Jae Woo Kim⁴, Derek W. Morris², Sinéad M. Waters^{2*}

1 Animal and Bioscience Research Department, Animal and Grassland Research and Innovation Centre, Teagasc, Grange, Meath, Ireland, **2** School of Biological and Chemical Sciences, University of Galway, Galway, Ireland, **3** Veterinary Sciences Division, Agri-Food and Biosciences Institute, Stormont, Belfast, Ireland, **4** Division of Animal Sciences, University of Missouri, Columbia, Missouri, United States of America,

* Sinead.Waters@universityofgalway.ie



OPEN ACCESS

Citation: O'Donoghue S, Earley B, Johnston D, Finnie MS, Cosby SL, Lemon K, et al. (2025) Examination of the lung and lymphoid tissue mRNA transcriptome response in dairy calves following experimental challenge with bovine alphaherpesvirus one (BoHV-1). *PLoS One* 20(5): e0319575. <https://doi.org/10.1371/journal.pone.0319575>

Editor: Gianmarco Ferrara, University of Messina: Università degli Studi di Messina, ITALY

Received: September 9, 2024

Accepted: February 4, 2025

Published: May 2, 2025

Copyright: © 2025 O'Donoghue et al. This is an open access article distributed under the terms of the [Creative Commons Attribution License](https://creativecommons.org/licenses/by/4.0/), which permits unrestricted use, distribution, and reproduction in any medium, provided the original author and source are credited.

Data availability statement: All sequence data generated in this study have been deposited in the NCBI Gene Expression Omnibus (GEO) repository (<https://www.ncbi.nlm.nih.gov/geo/>)

Abstract

Bovine alphaherpesvirus one (BoHV-1) is a primary cause of bovine respiratory disease (BRD), and a leading cause of morbidity and mortality in cattle. The transcriptomic responses of key respiratory and immune associated tissues of dairy calves following experimental challenge with BoHV-1 are unknown. Thus, the study objective was to examine the gene expression profiles of multiple tissue types from dairy calves following an infectious challenge with BoHV-1. Holstein-Friesian bull calves (mean age \pm SD 149.2 days \pm 23.8; mean weight \pm SD 174.6 kg \pm 21.3 kg) were challenged with either BoHV-1 inoculate (6.3×10^7 /mL \times 1.35mL) (n = 12) or sterile phosphate buffered saline (n = 6). Animals were euthanised on day 6 post-challenge and tissue samples collected, including bronchial (BLN) and mediastinal lymph nodes (MLN), pharyngeal tonsil (PGT) and healthy (HL) and lesioned right cranial lung (LL). Total RNA was extracted and libraries sequenced on an Illumina NovaSeq 6000. Differential expression analysis was conducted using edgeR and pathways analysed using DAVID. A weighted gene co-expression network analysis (WGCNA) was conducted separately for each tissue type to identify networks significantly associated with BoHV-1 infection. Differentially expressed genes (DEGs) were identified in all tissues (P < 0.05, FDR < 0.1, FC > 2). Thirty-three DEGs were common to all tissues and enriched pathways included Influenza A and Herpes simplex 1 infection (P < 0.05, FDR < 0.05). Modules enriched for antiviral and innate immune processes were identified for each tissue type. Of the 33 DEGs common to all tissues, 26 were also identified as hub genes in the blood (blue) module. Our use of a controlled experimental challenge allowed for improved understanding of the immune response

and are publicly available under the following accession numbers: GSE153242 (BLN data), GSE153429 (cranial lung lobe data), GSE227344 (PGT data), and GSE229115 (MLN data).

Funding: This project was funded by the Irish Department of Agriculture, Food and the Marine (DAFM) and the Department of Agriculture, Environment and Rural Affairs (DAERA), Northern Ireland, as part of the US-Ireland R&D partnership call (RMIS_0033 Project 16/RD/US-ROI/11). JT and JK were supported by Grant No. 2017-67015-26760 from the United States Department for Agriculture's National Institute for Food and Agriculture. There was no additional external funding received for this study.

Competing interests: The authors have declared that no competing interests exist.

of dairy calves to a BoHV-1 infection. Furthermore, discovering DEGs that are common to all tissues, including whole blood, indicates future focus areas in research surrounding BRD diagnostic biomarkers.

Introduction

Bovine respiratory disease (BRD) is a multifactorial syndrome affecting cattle of all ages in beef and dairy industries not only in Ireland [1,2] but internationally [3], often responsible for reduced animal performance and economic losses [4]. Stress resulting from management and environmental factors as well as infections caused by bacterial and viral agents influence the onset of BRD. A key BRD-associated virus, BoHV-1 is an *alphaherpesvirus* which causes the clinical disease infectious bovine rhinotracheitis (IBR) in cattle [5]. BoHV-1 has been shown to remain latent within the sensory neurons within trigeminal ganglia [6] and also in the pharyngeal tonsil of infected cattle [7]. As a result, despite recovering from acute infection, the dormant virus can reactivate causing the emergence of symptoms and viral shedding [8,9]. Although vaccines may reduce clinical symptoms of IBR, they have not been fully successful at preventing infection with BoHV-1 or the establishment of BoHV-1 latency [5].

Next-generation sequencing methodologies have been utilised in efforts to gain an improved understanding of the response of animals to infection by BRD pathogens at the molecular level. RNA sequencing (RNA-Seq) has been used to analyse the gene expression profiles of lung, pharyngeal tonsil, retropharyngeal lymph node, nasopharyngeal lymph node [10] and bronchial lymph node [11] in beef steers following experimental challenge with BoHV-1, resulting in the identification of key genes influencing the activation of key immune networks across lymphoid tissues. We have previously identified key biological pathways and processes such as inflammatory response, and viral pathways such as Influenza A and defence response to virus in the whole blood transcriptomes of calves experimentally challenged with BoHV-1 [12]. Furthermore, other studies have utilised a network-based approach to analyse the blood transcriptome profiles of cattle with BRD and have found networks and hub genes involved in the immune response to infection [13–15]. However, in these studies the BRD causal pathogen was unknown. One possible application for the discovery of important genes related to the immune response in whole blood is the creation of a BRD diagnostic that can be used “ante-mortem”.

The mechanisms by which BoHV-1 establishes infection and the host response to disease at the molecular level requires further study in weaned dairy calves. In particular, gene and network regulation in respiratory and immune tissues should be studied to complement findings in whole blood [12]. Studies focusing on pan-tissue transcriptomics in response to key pathogens allow for a better understanding of the immune system functionality at the molecular level. Furthermore, the use of network based approaches allows for the examination of interactions between genes governing a particular phenotypic outcome [16], and the identification of hub genes

involved in the regulation of other network genes, may enable the development of biomarkers for traits such as BRD [17]. Hub genes are highly connected genes within a co-expression module that help to explain the module functioning [14,18].

The objectives of this study were threefold; first, to characterise the gene expression profiles of key immune and respiratory associated tissues in dairy calves experimentally infected with BoHV-1 and identify the biological processes that are enriched. Second, to cross-analyse the DEGs identified with those previously identified in whole blood from the same animals in response to a BoHV-1 challenge [12]. Finally, to perform WGCNA on the analysed tissues augmented by the whole blood data from O'Donoghue *et al.* (2023) and to determine if any modules and associated pathways identified in the key respiratory and immune tissues are also detected in the blood.

Materials and methods

Animal model

All animal studies were carried out in accordance with the UK Animals (Scientific Procedures) Act 1986 and with the approval of the Agri-Food and Biosciences Institute Northern Ireland Ethical Review Committee. The details of the study have been reported in accordance with the ARRIVE guidelines (<https://arriveguidelines.org/>).

The model and sampling protocol used in this study have previously been described (O'Donoghue *et al.*, 2023). In brief, Holstein-Friesian bull calves (mean \pm SD age 149.2 \pm 23.82 days) were selected based on low BoHV-1 specific maternally derived antibody levels and negative BoHV-1 PCR status. Calves were either challenged with BoHV-1 inoculum (strain 2011-426) (dose = 6.3×10^7 /mL in a volume of 1.35mL per animal) (n = 12) or mock-challenged with sterile phosphate buffered saline (PBS) (n = 6). Clinical signs such as nasal discharge, ocular discharge, general demeanour, size of mandibular lymph nodes, presence of a cough, respiratory rate, respiratory character, mouth breathing, dyspnoea, presence of an expiratory grunt and rectal temperature were recorded daily from the day of challenge until euthanasia, and scores were calculated by a trained veterinarian blinded to the calves treatment status, using the scoring system described by Johnston *et al.* (2019). On day 6 post-challenge, calves were euthanised by captive bolt. At post-mortem, a trained veterinary pathologist examined and scored the lungs using an AFBI standardised scoring system, which assigns the percentages of lesions present on the total lung area and on component parts of the lungs. The workspace and implements were thoroughly cleaned and disinfected with bleach and 75% ethanol and sprayed with RNaseZap for RNase inhibition, before tissue collection and between the processing of each animal. Tissue samples BLN, MLN, PGT, HL and LL were harvested, immediately flash frozen in liquid nitrogen, and placed on dry ice before storage at -80°C . BoHV-1 viral load was assessed using qPCR and was performed on BLN, MLN, PGT and lung tissue samples (data not shown). BoHV1 PCR was performed using the exopol EXOone oneMIX BoHV-1 kit (exopol, Spain), according to the manufacturer's instructions.

RNA extraction

Total RNA was extracted using the Qiagen RNeasy Plus Universal Mini Kit (Qiagen LTD, Manchester, UK), according to the manufacturer's instructions. The quantity of the extracted RNA was determined by measuring the absorbance at 260nm with a Nanodrop spectrophotometer (Nano Drop technologies; Wilmington, DE, USA). The quality of the extracted RNA was examined with the Agilent 2100 Bioanalyzer (Agilent Technologies Ireland Ltd; Dublin, Ireland) using the RNA 6000 Nano LabChip kit (Agilent Technologies Ireland Ltd; Dublin, Ireland). The mean \pm SD RNA Integrity Number for BLN, MLN, PGT, HL and LL samples were 9.07 ± 0.11 , 9.32 ± 0.21 , 9.4 ± 0.17 , 8.83 ± 0.16 and 9.14 ± 0.30 respectively.

RNA-Seq library preparation and sequencing

RNA samples were shipped frozen at -80°C on dry ice to the University of Missouri's Genomics Technology Core (Columbia Missouri, USA). Library preparation was performed using the TruSeq stranded mRNA kit (Illumina, San Diego,

California, USA) and libraries sequenced (150 bp (BLN, lung) or 100 bp (MLN, PGT) paired-end) on an Illumina Nova-Seq 6000. All sequence data produced in this study have been deposited to the NCBI GEO repository and are available under the following accession codes: GSE153242 for BLN, GSE153429 for cranial lung lobe, GSE227344 for PGT and GSE229115 for MLN. Whole blood RNA-Seq data from O'Donoghue et al. (2023) are available at GEO with accession number GSE199108.

Read processing

Sequence reads were received in FASTQ format and were assessed for quality using FastQC (version 0.11.8). Reads were trimmed at the 3' end using cutadapt (version 1.18) [19] for the removal of short reads (< 10 bases), ambiguous nucleotides and poly-G-artefacts. Trimmed reads were then re-assessed using FastQC to ensure that all reads passed the basic quality statistics. Sequence reads were aligned to the ARS-UCD1.2 bovine reference genome [20] and read counts generated using the STAR (Spliced Transcripts Alignment to a Reference) alignment tool (version 2.6.1b).

Differential expression analysis

Raw read counts were input into R (version 4.3.2 (2023-10-31)) and differential expression analysis performed using the edgeR package (version 4.0.5) which uses an over-dispersed model to account for arising biological and technical variation [21]. Genes with less than one read count per million in the smallest number of samples per treatment were removed from the analysis. The trimmed-mean of M values method was used to normalise the data and the negative binomial dispersion parameters were estimated using the quantile-adjusted conditional maximum likelihood estimator. Differentially expressed (DE) genes between the treatment (control and challenged) groups were detected using exact tests, with genes considered DE if they had a Benjamini-Hochberg false discovery rate (FDR) of ≤ 0.1 and a fold change of ≥ 2 . To analyse the DEGs common across tissues, DEGs from each tissue type were input into the Venn diagram tool on BioTools.fr <https://www.biotoools.fr/misc/venny>. Genes common to all tissue types, which had the same direction of regulation (upregulated) between treatments were ranked using a methodology similar to that described by Laighneach et al. (2021) [22]. For each tissue, genes were ordered by statistical significance for DE and assigned a rank (with the most significant DEG ranked first). The rank for each DEG within each tissue type were then summed across tissues to produce a sum rank. A spearman correlation was performed using the cor() function in R (version 4.3.2 (2023-10-31)) to assess the relationship between viral load (qPCR data) and the common DEGs in each tissue type. Correlation (effect size and the strength of the correlation) was described using the following: 0.00–0.19 “very weak”; 0.20–0.39 “weak”; 0.40–0.59 “moderate”; 0.60–0.79 “strong”; 0.80–1.0 “very strong” [23,24].

Pathway and gene ontology analysis

For the detection of perturbed biological pathways and gene ontologies, DEGs were input into the Database for Annotation, Visualization and Integrated Discovery (DAVID) [25,26]. The lists of DEGs identified within each tissue type were separately uploaded to DAVID and Kyoto Encyclopaedia of Genes and Genomes (KEGG) and gene ontology (GO) terms for biological processes (BP), cellular components (CC) and molecular functions (MF) were interrogated. Pathways and ontologies with a $P \leq 0.05$ and $FDR \leq 0.05$ were considered enriched for DEGs. This analysis was also performed for the DEGs found to be common to all tissue types.

Gene co-expression analysis

For each tissue dataset, raw RNA-seq read counts were filtered for lowly expressed genes, by retaining only genes that had greater than one count per million in at least 12 samples (BoHV-1 challenged) or 6 samples (control). The filtered reads were normalised in edgeR using the trimmed mean of M – values normalisation method. Normalised counts were

then $\text{Log}_2(x + 1)$ transformed in R. Filtered reads were input into R and weighted gene co-expression network analysis (WGCNA) was performed on the data for each tissue type individually using the WGCNA R package (version 1.72-5) which identifies modules (or networks) of co-expressed genes [27]. First, a similarity matrix was constructed to estimate the similarity between genes with similar expression profiles. The similarity matrix was next transformed into an adjacency matrix using a soft thresholding power corresponding to $R^2 \geq 0.8$ [14]. The adjacency matrix, which encodes the strength of the connection between pairs of genes, was finally transformed into a topological overlap matrix (TOM) and the corresponding dissimilarity (distance) of genes was calculated to minimize the effects of noise and false associations [28]. Average linkage hierarchical clustering was applied to the TOM for each tissue dataset using the `hclust` function in R to produce a hierarchically clustered tree of genes for each tissue type. The `dynamicTreeCut` package (version 1.63-1) 10.32614/CRAN.package.dynamicTreeCut was then used to identify modules (groups of co-expressed genes). Module eigengenes were calculated using the `moduleEigengenes` function in the WGCNA package, to quantify the co-expression similarity of the entire module. Modules with genes possessing highly similar expression profiles were merged based on their correlation and assigned a colour identifier by the software [27].

Pearson's correlation was used to analyse the relationship between identified modules of co-expressed genes and selected clinical traits (treatment (BoHV-1-challenged), clinical score and rectal temperature). A positive Pearson correlation indicates that a module is associated with BoHV-1 infection and a negative Pearson correlation indicates that a module is not associated with BoHV-1 infection. Modules with statistically significant ($P \leq 0.05$) correlations were selected for further analysis as biologically interesting modules associated with BoHV-1 infection.

Identification of hub genes within modules of interest

The module membership (MM) can take a positive or negative value, indicating that genes are positively or negatively related to the module eigengene, respectively. Genes which have a MM value closer to an absolute value of 1 are highly connected to the other genes within a module (Langfelder and Horvath, 2008). We considered genes with $MM > 0.9$ to be hub genes [29]. Hub genes identified in the significant modules for each tissue data set were then cross-analysed against the identified DEGs to reveal the genes identified in both analyses.

Pathway analysis and functional enrichment of modules of interest

Pathway analysis was conducted on genes present in modules significantly associated with the examined traits (BoHV-1-challenged, clinical score and rectal temperature). To perform these analyses the list of genes from each significant module were input into DAVID. The databases queried through DAVID were the KEGG, GO_BP, GO_CC and GO_MF. DAVID employs Fisher's exact test to determine the enrichment of pathways and ontology terms. Significant pathways and terms were considered those with a P-value < 0.05 and FDR < 0.05 .

Protein-protein interaction (PPI) analysis

Genes that exist in close proximity to each other in a genome can have functional associations [30]. DEGs common to all tissue types were input into the search tool for recurring instances of neighbouring genes (STRING) (version 12.0) [30,31], for the examination of functional associations between their encoded proteins.

Results

Clinical scores, haematology variables and lung pathology

Clinical scores and lung pathology measures have been described previously [12]. Briefly, there was a significant treatment \times day (d) interaction for both clinical scores ($P < 0.05$) and rectal temperature ($P < 0.01$) between control and challenged calves, whereby clinical scores and rectal temperatures were greater for BoHV-1 challenged compared to

control calves on d 4, 5, and 6 post-challenge. BoHV-1 challenged calves had higher clinical scores ($P < 0.001$) and rectal temperatures ($P < 0.0001$) on d 3, 4, 5, and 6 relative to d -1. There were no differences in lung scores in the overall lung or the right cranial lung lobe lung between BoHV-1 challenged and control calves ($P > 0.05$).

Differential gene expression analysis

The mean sequence reads \pm SD obtained for the tissues were; 40,815,975 \pm 4,282,489 (BLN), 44,308,241 \pm 4,896,483 (MLN), 81,200,000 \pm 8,920,000 (PGT), 41,181,735 \pm 4,308,861 (HL) and 40,502,064 \pm 5,048,646 (LL) of which 94%, 86%, 86%, 94% and 94% of reads were uniquely aligned to the ARD UCD 1.2 bovine reference genome respectively.

There were 337, 81, 1833, 334, and 67 DEGs identified ($P < 0.05$, FDR < 0.1 , FC > 2) between control and challenged calves in the BLN, MLN, PGT, HL and LL samples respectively (S1 Table). Multi-dimensional scaling based on global gene expression, revealed a clear separation between the control and challenged groups in the BLN, PGT and HL (Supplementary Figures 1–5 S2 File). Multi-dimensional scaling of all samples based on global gene expression revealed four distinct clusters (Fig 1). The gene expression profiles of the whole blood and PGT separated into two distinct clusters. The MLN and BLN samples formed a cluster, as did samples from the LH and LL.

A Venn diagram was used to display the DEGs in common across tissue types (Fig 2). There were 35 DEGs common to all tissue types, and all were upregulated in response to BoHV-1 (S2 Table). Strikingly, thirty-three of these genes were also DE and upregulated in the whole blood data from O'Donoghue *et al.* (2023). Table 1 shows the sum ranks of p-values for these DEGs across all tissues with the lowest sum rank representing the most significant gene.

Significant relationships were found between the expression of these genes and the BoHV-1 viral load in the PGT and MLN, with 19 and 1 gene(s) moderately significantly correlated respectively (S1 File).

PPI analysis

An examination of the functional connections among the proteins encoded by the 33 genes common to all tissue types in STRING (version 12) revealed that this gene group had significantly more interactions than expected if the genes had been sampled at random ($P < 1.0e-16$). This suggests that these proteins are biologically connected as a group. A PPI network for these genes is presented in Fig 3 (S3 Table). Table 2 presents the STRING functional analysis of the PPI network.

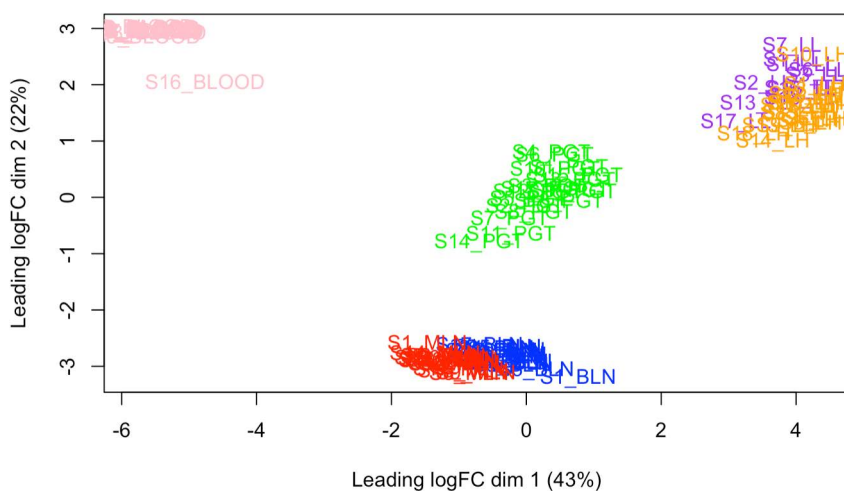


Fig 1. A multi-dimensional scaling plot based on all samples from each tissue type. Samples separated into four clusters; whole blood (pink), PGT (green), MLN and BLN (red and blue, respectively) and LH and LL (orange and purple, respectively).

<https://doi.org/10.1371/journal.pone.0319575.g001>

Table 1. The sum-ranked DEGs common across all tissue types (BLN, MLN, PGT, LH, LL and whole blood), in response to a BoHV-1 challenge in dairy calves. DEGs are ordered based on rank with the lowest ranked gene (most significant) listed first. Ensemble ID's, gene symbol and an associated function is shown for each gene.

ENSEMBLE ID	Gene Symbol	Associated Function	Sum Rank
ENSBTAG00000012406	ZBP1	An innate immune sensor involved in the activation of the interferon response [32]. Plays a role in the induction of inflammatory cell death (pyroptosis, apoptosis and necroptosis) [33].	49
ENSBTAG00000019018	IFITM3	Interferon inducible membrane protein that restricts viral infection [34].	54
ENSBTAG00000020166	ZNFX1	Encoded protein is a zinc finger protein involved in the innate and antiviral immune response [35].	55
ENSBTAG00000003366	RIGI	Involved in the recognition of viral RNA [36].	60
ENSBTAG000000053806	ENSBTAG000000053806	Upregulated in the bovine endometrium in response to interferon-tau [37].	60
ENSBTAG000000017367	IFIT5	Involved in innate and anti-viral immune responses [38].	65
ENSBTAG000000014628	OAS2	Interferon-induced gene with a vital role in the antiviral activity of interferons [39].	73
ENSBTAG000000030932	IFI44L	Involved in the negative modulation of innate immune response to viral infection. Excessive immune responses can be harmful to hosts, therefore negative feedback is needed [40].	77
ENSBTAG000000039861	OAS1Y	Interferon-induced gene with a vital role in the antiviral activity of interferons [39].	79
ENSBTAG000000037527	OAS1X	Interferon-induced gene with a vital role in the antiviral activity of interferons [39].	85
ENSBTAG000000046580	DHX58	Involved in the negative regulation of RIG-1 signalling and type 1 interferon production [41].	93
ENSBTAG000000020536	HERC6	Encodes proteins induced by type I interferons, and is upregulated in cattle with BRD [42].	97
ENSBTAG000000052306	ENSBTAG000000052306	Unknown	98
ENSBTAG000000019018	IFITM3	Interferon inducible membrane protein that restricts viral infection [34].	98
ENSBTAG000000008471	MX2	Involved in the innate immune response to viral infection [43].	99
ENSBTAG000000010057	GZMB	Encodes a member of the granzyme subfamily of proteins involved in the defence response to viral infection [44].	100
ENSBTAG000000025398	ENSBTAG000000025398	Amongst the most DE hub genes associated with intramuscular fat in Nellore cattle [45].	103
ENSBTAG000000011343	XAF1	Targets IRF7 to inhibit type 1 interferon production during viral infection [46].	107
ENSBTAG000000008021	ENSBTAG000000008021	DE in the endometrium of pregnant dairy cows 15 days after insemination [47].	110
ENSBTAG000000007554	IFI6	Involved in the negative modulation of innate immune response [48].	110
ENSBTAG000000045588	ENSBTAG000000045588	Function unknown; Upregulated in bovine endometrium explants in response to interferon-tau and conceptuses [49].	111
ENSBTAG000000003152	IFI27	Role in viral infections. Counterbalances the innate immune response to RNA viral infection [50].	111
ENSBTAG000000021565	PRSS2	Downregulated in Holstein-Friesian cell lines infected with <i>Theileria annulata</i> [51].	121
ENSBTAG000000030913	MX1	Interferon-induced protein with antiviral activities [52].	122
ENSBTAG000000008703	EIF2AK2	Encodes a serine/threonine kinase involved in type 1 interferon production and the regulation of transcription factors including NF- κ B and IRF-1 [53,54].	123

(Continued)

Table 1. (Continued)

ENSEMBLE ID	Gene Symbol	Associated Function	Sum Rank
ENSBTAG00000014707	<i>ISG15</i>	Interferon-induced ubiquitin like modifier with a role in the host response to viral infection [55].	123
ENSBTAG00000007881	<i>IFIT1</i>	Interferon stimulated gene involved in the innate immune response [56].	124
ENSBTAG00000016061	<i>RSAD2</i>	Interferon stimulated gene with role in the innate and antiviral immune responses [57].	133
ENSBTAG00000019979	<i>CMPK2</i>	Involved in inflammatory and viral respiratory disease [58]; Role in antitumor and antibacterial immunity [59].	136
ENSBTAG00000014529	<i>GBP4</i>	Upregulated in non-classical and intermediate monocytes in <i>Bos taurus</i> cattle [60]. GBP4 is a negative regulator of virus-triggered IFN-1 production through the targeting and inhibition of IRF7 [61].	138
ENSBTAG00000012335	<i>UBA7</i>	Involved in activating ISG15 for antiviral functioning [62].	139
ENSBTAG00000032265	<i>RTP4</i>	Involved in antiviral immune response [63].	151
ENSBTAG00000053807	ENSBTAG00000053807	DE in the endometrium of pregnant dairy cows 15 days after insemination [47].	162

<https://doi.org/10.1371/journal.pone.0319575.t001>

Pathway analysis of genes within modules

Analysis of the genes from each significant module for each tissue type through DAVID revealed enriched pathways and gene ontology terms ($P < 0.05$, $FDR < 0.05$). There were no significant KEGG pathways identified for the genes in significant modules in the BLN or MLN data. A list of the KEGG pathways enriched for significant modules in the PGT, LH, LL and whole blood data are provided in S16–S19 Tables, respectively.

The blue module identified for the blood, was significantly and positively associated with BoHV-1 infection. Many of the KEGG pathways enriched for the genes in this module were also enriched for genes in significant modules across the other tissue types. Fig 5 shows the KEGG pathways from this module that are also enriched in other tissue modules.

Hub gene identification and overlap with DEGs

Across all the tissue types, 3472 hub genes ($MM > 0.9$) were identified. A list of the hub genes identified for each tissue type is provided in S20 Table. The blue module identified in the blood analysis had many overlaps in enriched pathways with significant modules across other tissue types. Five hundred and seventeen hub genes ($MM > 0.9$) were identified in this module, with 125 also identified as DEGs by O'Donoghue *et al.* (2023). Of these, 26 were amongst the 33 genes common to all tissues (Fig 6), demonstrating that these genes are centrally important to the processes enriched in this module. A list of the hubs genes also found to be DE in each tissue type is provided in S21 Table.

Discussion

In the present study, DE and WGCNA approaches were used to analyse the transcriptome profiles of bronchial, and mediastinal lymph node, pharyngeal tonsil, healthy and lesioned lung and whole blood samples collected from dairy calves experimentally infected with BoHV-1. Previous studies by our groups have examined the transcriptome response of various tissue types from animals following a single pathogen challenge with BRD causative agents (Tizioto *et al.*, 2015; Behura *et al.*, 2017; Johnston *et al.*; 2019; Johnston *et al.*, 2021; O'Donoghue *et al.*; 2023). These studies used a functional genomics approach, RNA-Seq, to identify DEGs between different phenotypes (e.g., control versus infected animals). This methodology has been successful in uncovering genes and biological pathways involved in the host immune response to BRD, with our group identifying differentially regulated genes in response to experimental challenges with BRSV (Johnston *et al.*, 2019; Johnston *et al.*, 2021) and BoHV-1 (O'Donoghue *et al.*, 2023). The use of co-expression networks for the examination of correlation patterns

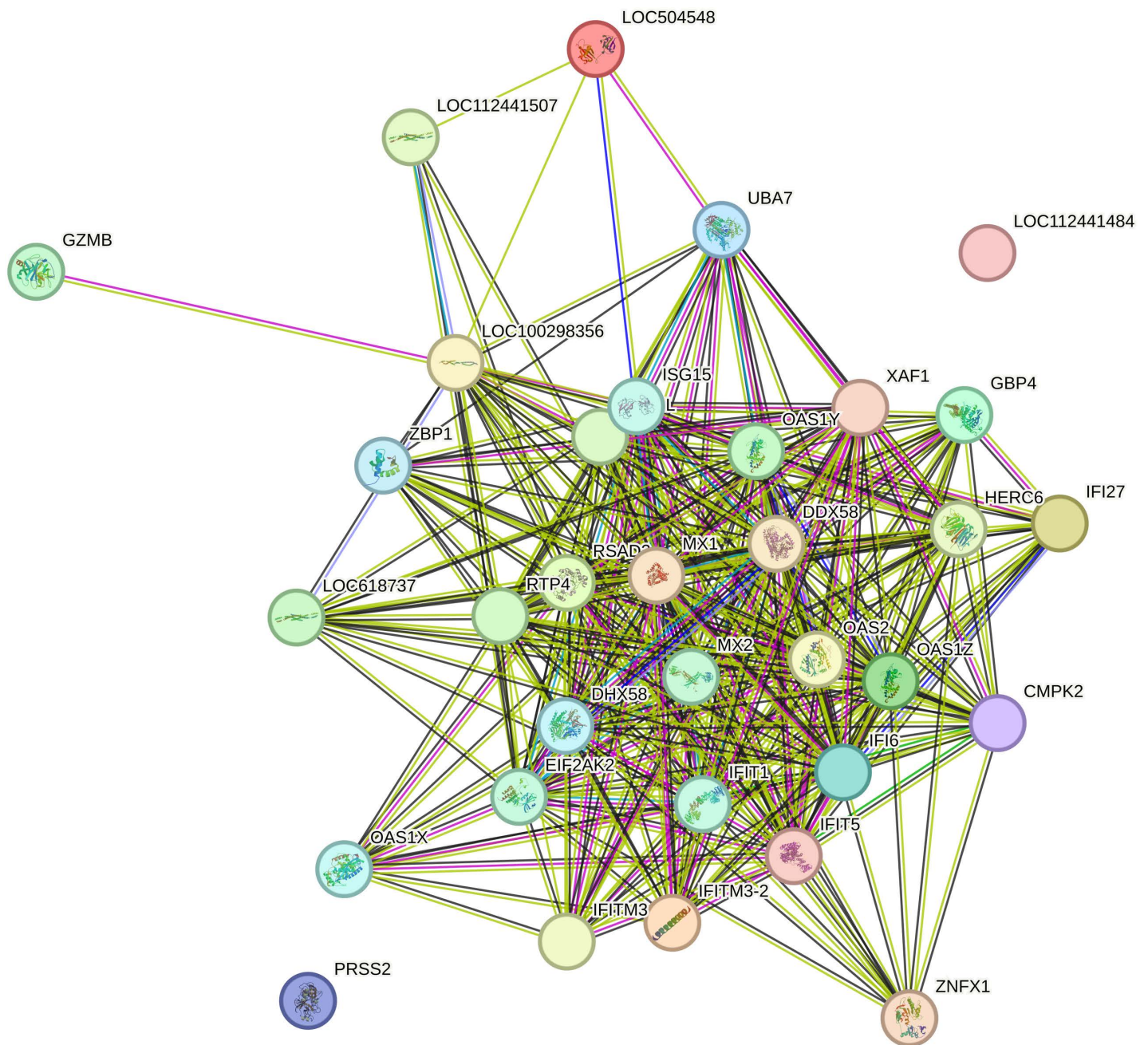


Fig 3. A PPI network for the 33 DEGs common to all tissue type. Nodes represent each protein where coloured nodes represent the first shell of interactors and white nodes represent second shell of interactors. Within some nodes the known or predicted 3D structure is given and in blank nodes the 3D structure of the protein is unknown. Edges represent the protein-protein associations and are colour coded; light blue = known interactions from curated databases, pink = known interactions determined experimentally, green = predicted interactions gene neighbourhood, red = predicted interaction gene fusion, dark blue = predicted interaction gene co-occurrence. The light green, black and lilac edges represent other interactions such as text mining, co-expression and protein homology respectively.

<https://doi.org/10.1371/journal.pone.0319575.g003>

Table 2. Functional analysis conducted in STRING for the 33 DEGs common across all tissue types.

Biological Process (Gene Ontology)				
Term/cluster no:	Description	Count in network	Strength	FDR
GO:0060700	Regulation of ribonuclease activity	4 of 9	2.47	1.56E-06
GO:0070106	interleukin-27-mediated signalling pathway	2 of 5	2.42	0.0135
GO:032020	ISG15-protein conjugation	2 of 6	2.34	0.0168
GO:0045071	Negative regulation of viral genome replication	14 of 45	2.31	2.03E-25
GO:0034340	Response to type I interferon	7 of 26	2.25	2.39E-11
Molecular Function (Gene Ontology)				
GO:0001730	2-5-oligoadenylate synthetase activity	4 of 5	2.72	1.5E-06
GO:0008191	Metalloendopeptidase inhibitor activity	3 of 17	2.07	0.0027
GO:0003725	Double-stranded RNA binding	7 of 73	1.8	1.03E-07
GO:003723	RNA binding	11 of 1191	0.79	0.00081
Cellular Component (Gene Ontology)				
GO:0005737	Cytoplasm	28 of 10284	0.26	0.0139
Local network cluster (STRING)				
CL:18979	Dynamin, GTPase and Host cell	5 of 5	2.82	5.70E-10
CL:18976	ISG15 antiviral mechanism, and TLD	7 of 10	2.67	7.54E-14
CL:18969	Negative regulation of viral genome replication and cellular response to interferon-alpha	14 of 21	2.65	1.51E-29
KEGG Pathways				
bta05160	Hepatitis C	10 of 150	1.65	8.7E-12
bta5164	Influenza A	10 of 160	1.62	8.7E-12
bta05162	Measles	8 of 136	1.59	3.85E-09
bta04622	RIG-I-like receptor signalling pathway	3 of 65	1.49	0.0069
bta05169	Epstein-Barr virus infection	7 of 197	1.37	1.59E-06
Reactome Pathways				
BTA-1169408	ISG15 antiviral mechanism	6 of 26	2.18	1.04E-08
BTA-936440	Negative regulators of DDX58/IFIH1 signalling	3 of 17	2.07	0.0014
BTA-168256	Immune system	8 of 802	0.82	0.0211
WikiPathways				
WP1017	Type II interferon signalling (IFNG)	4 of 30	1.95	4.61E-05
Tissue Expression (TISSUES)				
BTO:0000801	Macrophage	4 of 102	1.41	0.0211
BTO:0000089	Blood	6 of 427	0.97	0.0225
BTO:0000570	Hematopoietic system	14 of 1106	0.92	5.64E-07
BTO:0005810	Immune system	8 of 802	0.82	0.0211
Annotated Keywords (UniProt)				
KW-0051	Antiviral defence	6 of 51	1.89	1.25E-07
KW-0399	Innate immunity	5 of 113	1.47	0.00022

The term number provides a numerical reference to each term or pathway.

For each term, a description as well as the count in network is provided. The latter is a count of the number of genes from our data out of the total number of genes associated with that term.

The strength figure is the Log10 (observed/expected), and describes how large the enrichment is, based on the number of proteins in our network annotated with the term and the number of proteins expected to be annotated in a random network of the same size.

The FDR details the p-value for each term corrected for multiple testing using the Benjamini-Hochberg procedure.

<https://doi.org/10.1371/journal.pone.0319575.t002>

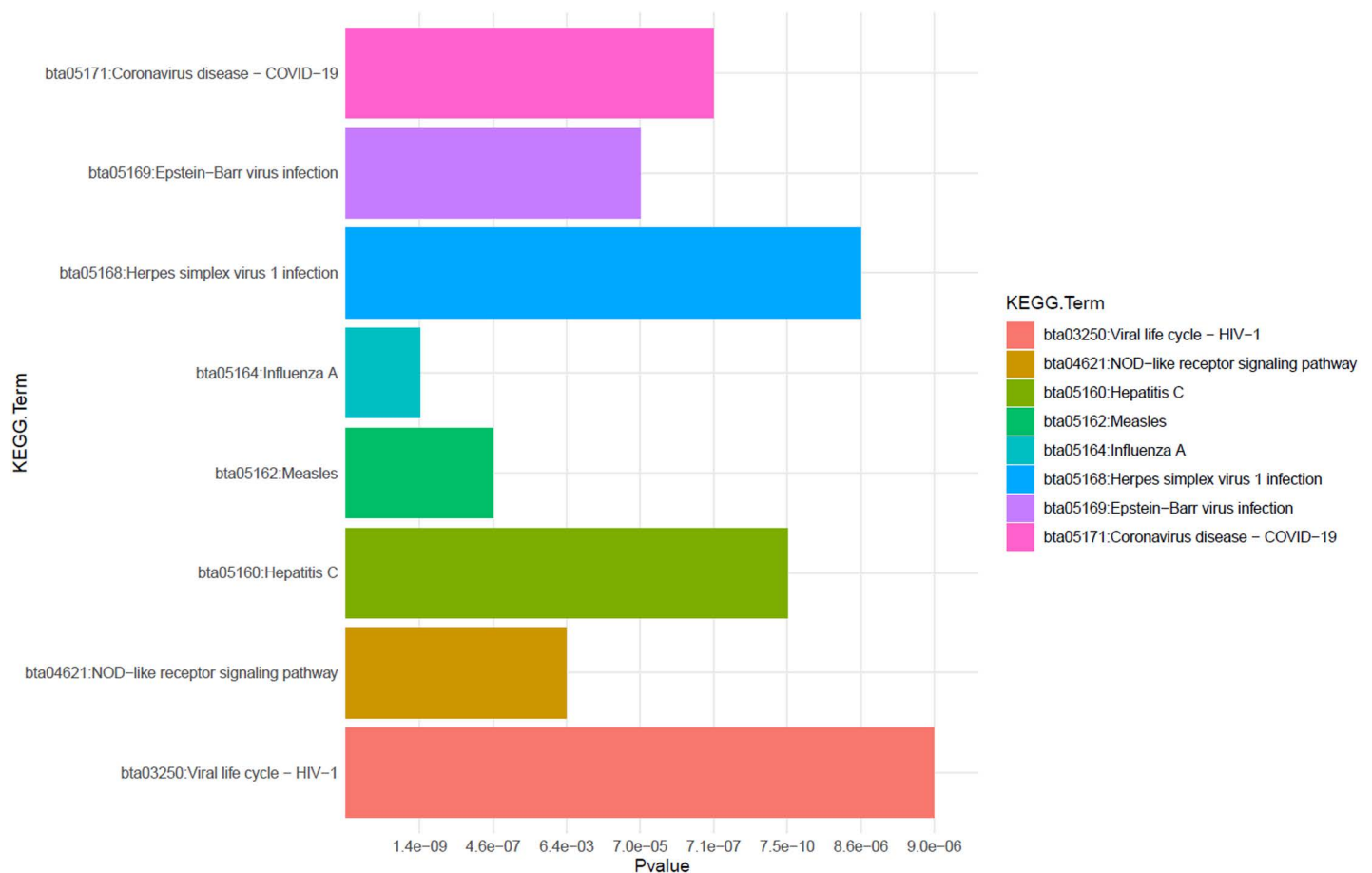


Fig 4. A bar plot displaying the KEGG pathways enriched for the DEGs common to all tissue types. The significance (P-value) for each term is given on the X-axis and the term name is given on Y-axis.

<https://doi.org/10.1371/journal.pone.0319575.g004>

across tissues to find clusters of highly correlated genes and regulatory genes within these networks is crucial [18,27], given that genes and gene products operate in association with many other genes, connected in larger, more complex networks. For example, Behura et al. (2017) utilised a network approach to identify key genes and networks enriched in various lung and lymphoid tissue in beef calves following experimental challenge with a range of viral and bacterial BRD causative agents. Other studies have utilised network-based analyses to investigate the regulatory networks in whole blood that may be involved in naturally contracted BRD infection [13–15]. In studies of naturally infected animals, clinical signs are often used as a means of BRD diagnosis, making it difficult to identify the causative agent and thus, the initial cause of infection.

We found 33 DEGs in common among all of the analysed tissues in response to BoHV-1 infection. The upregulation of all these genes in all tissues in response to infection suggests that they play a key role in mounting the across-tissue immune response to BoHV-1. Furthermore, the fact that these genes are also upregulated in circulating whole blood suggests that they may have potential as ‘ante-mortem’ biomarkers of BRD, allowing earlier diagnosis of BoHV-1 infection. Many of these genes (*DHX58*, *EIF2AK2*, *GZMB*, *IFI44L*, *IFI6*, *IFITM3*, *ISG15*, *MX1*, *MX2*, *OASIY*, *OAS2* and *RSAD2*) were also identified as hub-hub genes in the whole blood of cattle with BRD and were suggested to be critical in the immune response to BRD infections [14]. Further, Johnston et al. (2019) found several of these genes (*EIF2AK2*, *IFIT1*, *IFIT5*, *ISG15*, *MX1*, *OAS2* and *RSAD2*) to be DE in the bronchial lymph node of dairy calves following an experimental challenge with BRSV [64]. A study analysing the bronchial lymph node transcriptome profiles of beef cattle following single pathogen

Blood Blue module KEGG terms	PGT	LH	LL
Protein processing in endoplasmic reticulum	Darkorange2 (2.8E-24)		
N-Glycan biosynthesis	Darkorange2 (1.2E-08)		
Epstein-Barr virus infection		Seagreen3 (3.3E-18)	
Viral protein interaction with cytokine and cytokine receptor	Darkorange2 (2.7E-14)	Seagreen3 (6.1E-10)	
NOD-like receptor signalling pathway		Seagreen3 (2.1E-12)	
Proteasome			
Phagosome	Darkorange2 (1.9E-09)		
Apoptosis			
Protein export			
Influenza A	Darkorange2 (7.4E-09)	Seagreen3 (2.3E-12)	Indianred (1.8E-06)

Fig 5. A matrix detailing the overlap of KEGG pathways enriched for genes in the blue module of the blood and the other tissues. Each KEGG term is listed on the left with the tissue codes given across the top of each column. The green squares represent the terms from the blue module that overlap in that tissue type. The module within each tissue is given in each green square as well as their respective P-value (in brackets).

<https://doi.org/10.1371/journal.pone.0319575.g005>

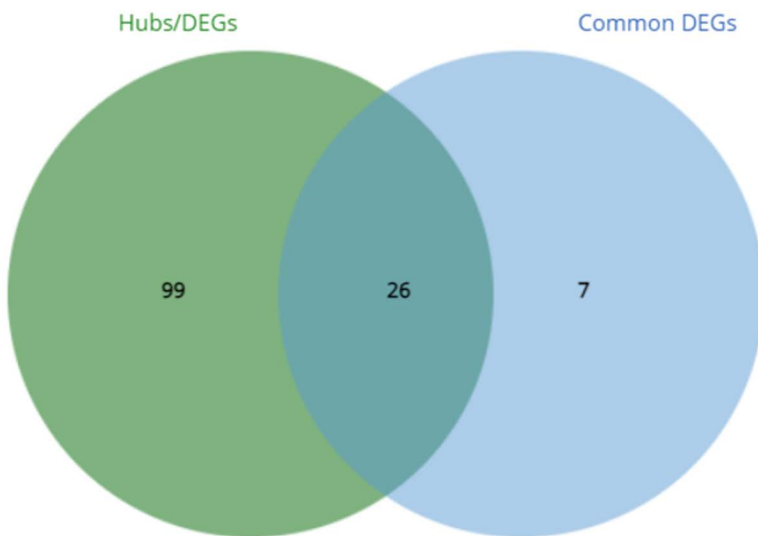


Fig 6. A Venn diagram showing the overlap of genes from the blood blue module identified as hubs and DEGs with those common across all tissue types.

<https://doi.org/10.1371/journal.pone.0319575.g006>

challenges with a range of BRD associated bacterial and viral pathogens also found some of these genes (*HERC6*, *ZBP1*, *IFIT1*, *ISG15* and *RSAD2*) to be DE in response to all challenge pathogens [11]. These findings also support the utility of these genes as potential biomarkers for the presence of BRD infection. Scott et al. (2022a) discussed the potential of rapid diagnostics for testing cattle for BRD upon arrival to the feedlot. Whole blood, as a tissue source, would be ideal for this

application as collection is relatively non-invasive, economical and practical [65]. Moreover, the usage of antibiotics in herds might potentially be decreased with testing, which has applications in both the dairy and beef industries.

The blue module identified in the whole blood data was enriched for several KEGG pathways that were also activated in some of the other tissue types. The pathways for N-glycan biosynthesis and protein processing in the endoplasmic reticulum were enriched in this module and were also enriched for module genes identified for the PGT. Glycans are an essential part of cell-cell interactions and N-glycans have been described as fine-tuners of immunological responses and potential molecular targets for the manipulation of immune tolerance and activation in a wide range of diseases and pathological conditions [66]. N-glycans, although involved in the immune response, can also be involved in viral attachment and entry to cells [67].

Analysis of the clinical scores found differences between the BoHV-1 challenged and control calves, as previously described [12]. Disease severity was not included as a variable in the DE analysis, representing a possible study limitation. However, clinical score was included in the WGCNA with the *antiquewhite2* and *sienna3* module significantly correlated with this trait in the BLN and MLN tissues respectively. Despite being significantly correlated, no KEGG pathways or ontology terms were enriched for the genes or hub genes in either module.

The pathways for 'Cytokine-cytokine receptor interaction' and 'Viral protein interaction with cytokine and cytokine receptor' were the most significant for DEGs in the PGT and were also enriched for genes in modules identified in the blood, LH and PGT. Cytokines are non-structural proteins, which play a regulatory role in processes such as inflammation, immunity and haematopoiesis [68], and often act as protectors against dangerous stimuli such as invading pathogens [69]. As a strategy to evade the host immune response, large DNA viruses, such as herpesviruses, encode homologues of cytokines, chemokines and their receptors [70], targeting chemokine-signalling networks to disrupt immune surveillance and defence of vertebrates [71]. The molecular mimicry of cytokines and cytokine receptors is known to be an immune modulation strategy adopted by herpesviruses [71]. Glycoprotein G (gG) is encoded in alphaherpesviruses and homologues of gG were found in BoHV-1 [72]. Recombinant gG from BoHV-1 was found to bind to a broad range of chemokines with high affinity and inhibit their biological activity *in vitro* [73]. These findings illuminate the nature of host-virus interactions occurring during BoHV-1 infection.

The most highly upregulated gene across all tissues analysed in the current study was *PRSS2* or serine protease 2. This gene was identified as the second most upregulated gene in whole blood in response to BoHV-1 [12]. Serine proteases are involved in a diverse range of biological processes including cellular and humoral immunity [74]. Other serine protease genes have been found to be differentially regulated in BRD cases with *PRSS45* downregulated in feedlot cattle at arrival that went on to develop BRD [75] while *PRSS50* was upregulated in feedlot cattle with BRD [76]. In humans, *PRSS2* is involved in inflammatory diseases [77,78] as well as tumour growth [79]. A recent study found that *PRSS2* is a key gene involved the regulation of lipid metabolism in dairy cows [80]. We found *PRSS2* to be amongst the DEGs involved in the protein digestion and absorption pathway in addition to several collagen genes that were downregulated in the bronchia lymph node, which may suggest it plays a role in collagen degradation. Additionally, we found this gene was also involved in the Influenza A pathway in other tissues. The significant upregulation of this gene across all our datasets in response to BoHV-1 infection suggests that it plays a key role in response BoHV-1 infection in dairy calves, and further investigation of its mechanism of action is warranted. Validation of key DEGs through qRT-PCR would strengthen the claim that these genes are central to the immune response to BoHV-1 infection, and we acknowledge that the absence of this validation could be a study limitation. Several pathways related to various viral infections such as Influenza A and Herpes Simplex infection were also identified. The Herpes Simplex infection pathway was enriched for the DEGs common to all tissue types as well as for genes in several significant modules. BoHV-1 and HSV1 share several biological properties, with both initiating infection in mucosal surfaces [81] and both are able to establish latency in the host sensory neurons [82]. DEGs and the gene modules involved in this pathway provide insight into the genes associated with the response to BoHV-1 infection.

Upon infection, pathogens express molecules known as pathogen-associated molecular patterns, which are recognised by host sensors called pathogen recognition receptors [83]. Nucleotide-binding oligomerization domain-like receptors (NLRs) are one such family of these receptors involved in the host response to BRD [84] and play a critical role in pathogen recognition and immune signalling [85]. Retinoic acid-inducible gene I (RIG-I) like receptors are RNA sensors crucial in innate antiviral immunity [86] and the detection of viral replication in the cytoplasm during early infection [87]. The NLR and RIG-I-like receptor signalling pathways were enriched for the DEGs common to all tissue types, suggesting that they play a role in the cross-tissue host response to infection, a finding similar to that of Behura et al. (2017). With their role in innate and adaptive immunity, and their influence on downstream signalling pathways, NLRs have been suggested as targets for therapeutic strategies for auto-inflammatory disorders [88]. In humans certain micro-RNAs have been shown to promote RIG-I-like signalling and enhance the antiviral immune response to certain viruses [89]. Genes involved in these pathways may serve as potential targets for BRD therapies.

Respiratory disease causing viruses often spread to the mediastinal lymph nodes from the lungs [90,91]. Of the identified DEGs, 11 were unique to this tissue type. Of these, the antimicrobial peptides *CATHL2* and *PGLYRP1* were also found to be upregulated in Holstein-Friesian cows with clinical mastitis [92]. The *AGRN* gene was also found to be uniquely upregulated in the MLN and a hypothesis surrounding its role in immune system regulation depicts that agrin expression in T cells may be upregulated during pathogenic infection and plays a role in cell-cell adhesion that is required for successful T cell activation [93]. The serine protease *PRSS45* was uniquely DE in the MLN and was found to be downregulated in the current study. Interestingly, this gene was found to be upregulated in the whole blood of cattle that had resisted BRD infection [75]. To our knowledge, this is the first study to examine the transcriptomic changes in the mediastinal lymph node in response to a BoHV-1 challenge in dairy calves.

We found the pharyngeal tonsil to possess the greatest number of DEGs in response to BoHV-1 infection, with 1833 genes DE. Further examination of these DEGs, revealed that 1573 (~ 86%) were unique to the PGT. The IL-17 signalling pathway was one of the most significant for the unique DEGs. Although we did not find an altered expression of *IL-17* in this tissue, we did detect the downregulation of both *IL17RE* and *IL17A*. In early stages of the host response to a virus, the host immune system induces the production of interferons and pro-inflammatory cytokines [94]. IL-17, which is primarily produced by $\gamma\delta$ T cells and CD4 + or Th17 cells [95], is a 'master regulator' of downstream cytokine and chemokine activities [96] and plays a key role in the maintenance of tissue integrity and the induction of protective immune responses to pathogens, particularly at epithelial barrier sites [97]. An increase in the expression of IL-17 was observed in the lungs of calves infected with the BRD-associated virus, BRSV [96]. Although a critical component of the host defence to viral infections, it has also been thought to play a role in the promotion of viral infection and related illness [98]. The ontology term for interleukin-27-mediated signalling pathway was also found to be enriched in the STRING analysis of the 33 DEGs common to all tissues. Interestingly, IL-17 has become a major drug target in a range of autoimmune and inflammatory diseases [99], and so could have potential as a target for BRD therapies.

The pathway for protein digestion and absorption was enriched in the BLN and many of the DEGs involved in this pathway (*ATP1A2*, *COL5A3*, *ELN*, *COL21A1*, *COL4A1*, *COL4A2*, *COL3A1*, *COL5A1* and *COL8A1*) were unique to this tissue type. All of these genes were found to be downregulated in response to BoHV-1 infection. A link exists between the extracellular matrix (ECM) and innate and adaptive immunity and the degradation and deposition of collagen is related to immune cell activity [100]. Collagen degradation in the extracellular matrix is known to result from tissue damage during infection and can enhance inflammation [100]. Interestingly, degraded collagen has also shown to be a chemoattractant for immune cells [101]. The unique differential expression of these genes in the BLN suggest this tissue to be involved in a specific aspect of the overall immune response to BoHV-1.

The right cranial lung lobes are a primary site for lesion development during BoHV-1 infection. Despite appearing healthy, we were able to identify over 300 DEGs in the LH, of which 130 were unique to this tissue. Genes in the phospholipase A2 group (*PLAG27* and *PLA2G2D5*) were found to be unique to this tissue and were upregulated in response

to BoHV-1. Phospholipases are enzymes responsible for the cleavage of ester bonds within phospholipids [102] and have been shown to play a role in host defence against bacteria, parasites and viruses [103]. *IRF9* was also uniquely upregulated in the healthy lung and is involved in virus-mediated activation of interferon [104]. In humans, it was found that mutations in *IRF9* resulted in increased susceptibility to viral infection and that *IRF9* deficient cells were unable to induce multiple interferon-stimulated genes (ISGs) [105]. This could suggest that *IRF9* plays a role in the regulation of ISGs in the lung during BoHV-1 infection.

Conclusion

Our use of a controlled experimental challenge allowed for an improved understanding of the specific immune responses to BoHV-1. Building on the work of others in this field, this study has successfully identified DEGs and important gene networks associated with BoHV-1 infection. *PRSS2* was found to be highly upregulated in all analysed tissues and therefore warrants further investigation into its role in BoHV-1 infection. A better understanding of the biological mechanisms underlying the host response to BoHV-1 was made possible by the application of a systems biology approach as opposed to a DE analysis alone. The discovery of DEGs that are present in all tissue types, including whole blood, suggests prospective future targets for BRD therapies and diagnostics.

Supporting information

S1 Table. A list of the DEGs identified for each tissue type.

(XLSX)

S2 Table. A list of the DEGS in each section of the VENN diagram.

(XLSX)

S3 Table. A PPI network of the 33 DEGS common to all tissue types.

(XLSX)

S4 Table. The DAVID results for the BLN tissue.

(XLSX)

S5 Table. The DAVID results for the MLN tissue.

(XLSX)

S6 Table. The DAVID results for the PGT tissue.

(XLSX)

S7 Table. The DAVID results for the HL tissue.

(XLSX)

S8 Table. The DAVID results for the LL tissue.

(XLSX)

S9 Table. The DAVID results for the 33 DEGs common to all tissues.

(XLSX)

S10 Table. A list of the genes in the significant modules in the BLN.

(XLSX)

S11 Table. A list of the genes in the significant modules in the MLN.

(XLSX)

S12 Table. A list of the genes in the significant modules in the PGT.

(XLSX)

S13 Table. A list of the genes in the significant modules in the LH.

(XLSX)

S14 Table. A list of the genes in the significant modules in the LL.

(XLSX)

S15 Table. A list of the genes in the significant modules in the blood.

(XLSX)

S16 Table. Enriched KEGG pathways for genes in the significant modules in the PGT.

(XLSX)

S17 Table. Enriched KEGG pathways for genes in the significant modules in the LH.

(XLSX)

S18 Table. Enriched KEGG pathways for genes in the significant modules in the LL.

(XLSX)

S19 Table. The DAVID results for genes in the significant modules in the blood.

(XLSX)

S20 Table. The hub genes identified for each tissue type.

(XLSX)

S21 Table. A list of the hubs genes also found to be DE in each tissue type.

(XLSX)

S1 File. Spearman correlation results.

(XLSX)

S2 File. Figures 1-5. MDS plots from the DE analysis performed for each tissue type.

(DOCX)

S6 Figure. Module trait association heatmaps for the modules detected in each tissue type (A = BLN, B = MLN, C = PGT, D = HL, E = LL and F = Blood). The module-trait relationships were colour coded based on correlation between the module and trait with red = strong positive correlation and green = strong negative correlation. The correlation coefficient and p- value (in parentheses) are given for each association. The traits are listed along the X-axis (treatment, clinical score and rectal temperature) and each module colour is given on the Y-axis.

(TIF)

Acknowledgements

Thanks is given to Dr Catherine Duffy in AFBI for assisting with the animal experiments.

Author contributions

Conceptualization: Bernadette Earley, Dayle Johnston, Matthew S. Finnie, S. Louise Cosby, Ken Lemon, Jeremy F. Taylor, Jae Woo Kim, Sinéad M. Waters.

Data curation: Stephanie O'Donoghue, Dayle Johnston, Matthew S. Finnie, S. Louise Cosby, Jeremy F. Taylor, Jae Woo Kim.

Formal analysis: Stephanie O'Donoghue, Dayle Johnston.

Funding acquisition: Bernadette Earley, Jeremy F. Taylor, Sinéad M. Waters.

Investigation: Stephanie O'Donoghue, Bernadette Earley, Dayle Johnston, Matthew S. Finnie, S. Louise Cosby.

Methodology: Stephanie O'Donoghue, Bernadette Earley, Dayle Johnston, Matthew S. Finnie, S. Louise Cosby, Ken Lemon, Michael J. McMenamy, Jae Woo Kim, Derek W. Morris, Sinéad M. Waters.

Project administration: Sinéad M. Waters.

Supervision: Bernadette Earley, Derek W. Morris.

Visualization: Stephanie O'Donoghue.

Writing – original draft: Stephanie O'Donoghue.

Writing – review & editing: Stephanie O'Donoghue, Bernadette Earley, Dayle Johnston, Matthew S. Finnie, S. Louise Cosby, Ken Lemon, Michael J. McMenamy, Jeremy F. Taylor, Jae Woo Kim, Derek W. Morris, Sinéad M. Waters.

References

1. Murray GM, More SJ, Sammin D, Casey MJ, McElroy MC, O'Neill RG, et al. Pathogens, patterns of pneumonia, and epidemiologic risk factors associated with respiratory disease in recently weaned cattle in Ireland. *J Vet Diagn Invest.* 2017;29(1):20–34. <https://doi.org/10.1177/1040638716674757> PMID: [28074713](https://pubmed.ncbi.nlm.nih.gov/28074713/)
2. Cuevas-Gómez I, McGee M, Sánchez JM, O'Riordan E, Byrne N, McDanel T, et al. Association between clinical respiratory signs, lung lesions detected by thoracic ultrasonography and growth performance in pre-weaned dairy calves. *Ir Vet J.* 2021;74(1):7. <https://doi.org/10.1186/s13620-021-00187-1> PMID: [33766106](https://pubmed.ncbi.nlm.nih.gov/33766106/)
3. Dubrovsky SA, Van Eenennaam AL, Karle BM, Rossitto PV, Lehenbauer TW, Aly SS. Epidemiology of bovine respiratory disease (BRD) in preweaned calves on California dairies: The BRD 10K study. *J Dairy Sci.* 2019;102(8):7306–19. <https://doi.org/10.3168/jds.2018-14774> PMID: [31202655](https://pubmed.ncbi.nlm.nih.gov/31202655/)
4. Peel DS. The effect of market forces on bovine respiratory disease. *Vet Clin North Am Food Anim Pract.* 2020;36(2):497–508. <https://doi.org/10.1016/j.cvfa.2020.03.008> PMID: [32451038](https://pubmed.ncbi.nlm.nih.gov/32451038/)
5. Muylkens B, Thiry J, Kirten P, Schynts F, Thiry E. Bovine herpesvirus 1 infection and infectious bovine rhinotracheitis. *Vet Res.* 2007;38(2):181–209. <https://doi.org/10.1051/vetres:2006059> PMID: [17257569](https://pubmed.ncbi.nlm.nih.gov/17257569/)
6. Jones C. Bovine herpesvirus 1 counteracts immune responses and immune-surveillance to enhance pathogenesis and virus transmission. *Frontiers in Immunology.* 2019;10.
7. Toomer G, Workman A, Harrison K, Stayton E, Hoyt P, Jones C. Stress triggers expression of bovine herpesvirus 1 infected cell protein 4 (bICP4) RNA during early stages of reactivation from latency in pharyngeal tonsil. *J Virol.* 2022;96(23):e01010-22.
8. Castrucci G, Cilli V, Frigeri F, Ferrari M, Ranucci S, Rampichini L. Reactivation of Bovid herpesvirus 1 and 2 and parainfluenza-3 virus in calves latently infected. *Comp Immunol Microbiol Infect Dis.* 1983;6(3):193–9. [https://doi.org/10.1016/0147-9571\(83\)90010-3](https://doi.org/10.1016/0147-9571(83)90010-3) PMID: [6313287](https://pubmed.ncbi.nlm.nih.gov/6313287/)
9. Winkler M, Doster A, Jones C. Persistence and reactivation of bovine herpesvirus 1 in the tonsils of latently infected calves. *J Virol.* 2000;74(11):5337–46.
10. Behura SK, Tizioto PC, Kim J, Grupioni NV, Seabury CM, Schnabel RD, et al. Tissue tropism in host transcriptional response to members of the bovine respiratory disease complex. *Sci Rep.* 2017;7(1):17938. <https://doi.org/10.1038/s41598-017-18205-0> PMID: [29263411](https://pubmed.ncbi.nlm.nih.gov/29263411/)
11. Tizioto PC, Kim J, Seabury CM, Schnabel RD, Gershwin LJ, Van Eenennaam AL, et al. Immunological response to single pathogen challenge with agents of the bovine respiratory disease complex: an rna-sequence analysis of the bronchial lymph node transcriptome. *PLoS One.* 2015;10(6):e0131459. <https://doi.org/10.1371/journal.pone.0131459> PMID: [26121276](https://pubmed.ncbi.nlm.nih.gov/26121276/)
12. O'Donoghue S, Earley B, Johnston D, McCabe M, Kim J, Taylor J, et al. Whole blood transcriptome analysis in dairy calves experimentally challenged with bovine herpesvirus 1 (BoHV-1) and comparison to a bovine respiratory syncytial virus (BRSV) challenge. *Frontiers in Genetics.* 2023;14.
13. Sun H-Z, Srithayakumar V, Jimenez J, Jin W, Hosseini A, Raszek M, et al. Longitudinal blood transcriptomic analysis to identify molecular regulatory patterns of bovine respiratory disease in beef cattle. *Genomics.* 2020;112(6):3968–77. <https://doi.org/10.1016/j.ygeno.2020.07.014> PMID: [32650099](https://pubmed.ncbi.nlm.nih.gov/32650099/)
14. Hasankhani A, Bahrami A, Sheybani N, Fatehi F, Abadeh R, Ghaem Maghami Farahani H. Integrated network analysis to identify key modules and potential hub genes involved in bovine respiratory disease: A systems biology approach. *Frontiers in Genetics.* 2021;12.

15. Scott MA, Woolums AR, Swiderski CE, Finley A, Perkins AD, Nanduri B, et al. Hematological and gene co-expression network analyses of high-risk beef cattle defines immunological mechanisms and biological complexes involved in bovine respiratory disease and weight gain. *PLoS One*. 2022;17(11):e0277033. <https://doi.org/10.1371/journal.pone.0277033> PMID: 36327246
16. Kogelman LJ, Cirera S, Zhernakova DV, Fredholm M, Franke L, Kadarmideen HN. Identification of co-expression gene networks, regulatory genes and pathways for obesity based on adipose tissue RNA Sequencing in a porcine model. *BMC medical genomics*. 2014;7:1–16.
17. Keogh K, Kenny DA. Gene co-expression networks contributing to reproductive development in holstein-friesian bull calves. *Animal*. 2022;16(5):100527. <https://doi.org/10.1016/j.animal.2022.100527> PMID: 35500509
18. van Dam S, Vösa U, van der Graaf A, Franke L, de Magalhães JP. Gene co-expression analysis for functional classification and gene-disease predictions. *Brief Bioinform*. 2018;19(4):575–92. <https://doi.org/10.1093/bib/bbw139> PMID: 28077403
19. Martin M. Cutadapt removes adapter sequences from high-throughput sequencing reads. *Bioinformatics*. 2011;17(1):3. <https://doi.org/DOIHere>
20. Rosen BD, Bickhart DM, Schnabel RD, Koren S, Elsik CG, Tseng E, et al. De novo assembly of the cattle reference genome with single-molecule sequencing. *Gigascience*. 2020;9(3):giaa021. <https://doi.org/10.1093/gigascience/giaa021> PMID: 32191811
21. Robinson MD, McCarthy DJ, Smyth GK. edgeR: A bioconductor package for differential expression analysis of digital gene expression data. *Bioinformatics*. 2010;26(1):139–40. <https://doi.org/10.1093/bioinformatics/btp616> PMID: 19910308
22. Laigneac A, Desbonnet L, Kelly JP, Donohoe G, Morris DW. Meta-analysis of brain gene expression data from mouse model studies of maternal immune activation using poly(I:C). *Genes (Basel)*. 2021;12(9):1363. <https://doi.org/10.3390/genes12091363> PMID: 34573345
23. Evans J. *Straightforward statistics for the behavioral sciences*. Thomson Brooks/Cole Publishing Co; 1996.
24. Papageorgiou SN. On correlation coefficients and their interpretation. *J Orthod*. 2022;49(3):359–61. <https://doi.org/10.1177/14653125221076142> PMID: 36017900
25. Huang DW, Sherman BT, Lempicki RA. Bioinformatics enrichment tools: paths toward the comprehensive functional analysis of large gene lists. *Nucleic Acids Res*. 2009;37(1):1–13. <https://doi.org/10.1093/nar/gkn923> PMID: 19033363
26. Huang DW, Sherman BT, Lempicki RA. Systematic and integrative analysis of large gene lists using DAVID bioinformatics resources. *Nat Protoc*. 2009;4(1):44–57. <https://doi.org/10.1038/nprot.2008.211> PMID: 19131956
27. Langfelder P, Horvath S. WGCNA: An R package for weighted correlation network analysis. *BMC Bioinformatics*. 2008;9:559. <https://doi.org/10.1186/1471-2105-9-559> PMID: 19114008
28. Zhang B, Horvath S. A general framework for weighted gene co-expression network analysis. *Statist Appl Genetics Mole Biol*. 2005;4(1):Article17.
29. Horvath S, Dong J. Geometric interpretation of gene coexpression network analysis. *PLoS Comput Biol*. 2008;4(8):e1000117. <https://doi.org/10.1371/journal.pcbi.1000117> PMID: 18704157
30. Snel B, Lehmann G, Bork P, Huynen MA. STRING: a web-server to retrieve and display the repeatedly occurring neighbourhood of a gene. *Nucleic Acids Res*. 2000;28(18):3442–4. <https://doi.org/10.1093/nar/28.18.3442> PMID: 10982861
31. Szklarczyk D, Kirsch R, Koutrouli M, Nastou K, Mehryary F, Hachilif R, et al. The STRING database in 2023: protein-protein association networks and functional enrichment analyses for any sequenced genome of interest. *Nucleic Acids Res*. 2023;51(D1):D638–46. <https://doi.org/10.1093/nar/gkac1000> PMID: 36370105
32. Upton JW, Kaiser WJ, Mocarski ES. DAI/ZBP1/DLM-1 complexes with RIP3 to mediate virus-induced programmed necrosis that is targeted by murine cytomegalovirus vIRA. *Cell Host Microbe*. 2012;11(3):290–7. <https://doi.org/10.1016/j.chom.2012.01.016> PMID: 22423968
33. Hao Y, Yang B, Yang J, Shi X, Yang X, Zhang D, et al. ZBP1: a powerful innate immune sensor and double-edged sword in host immunity. *Int J Mol Sci*. 2022;23(18):10224. <https://doi.org/10.3390/ijms231810224> PMID: 36142136
34. Smith S, Weston S, Kellam P, Marsh M. IFITM proteins-cellular inhibitors of viral entry. *Curr Opin Virol*. 2014;4:71–7. <https://doi.org/10.1016/j.coviro.2013.11.004> PMID: 24480526
35. Wang G, Zheng C. Zinc finger proteins in the host-virus interplay: multifaceted functions based on their nucleic acid-binding property. *FEMS Microbiol Rev*. 2021;45(3):fuaa059. <https://doi.org/10.1093/femsre/fuaa059> PMID: 33175962
36. Chan YK, Gack MU. RIG-I-like receptor regulation in virus infection and immunity. *Curr Opin Virol*. 2015;12:7–14. <https://doi.org/10.1016/j.coviro.2015.01.004> PMID: 25644461
37. O'Callaghan E, Sánchez JM, Rabaglino MB, McDonald M, Liu H, Spencer TE, et al. Influence of sire fertility status on conceptus-induced transcriptional response of the bovine endometrium. *Front Cell Dev Biol*. 2022;10:950443. <https://doi.org/10.3389/fcell.2022.950443> PMID: 36072344
38. Zhang B, Liu X, Chen W, Chen L. IFIT5 potentiates anti-viral response through enhancing innate immune signaling pathways. *Acta Biochim Biophys Sin (Shanghai)*. 2013;45(10):867–74. <https://doi.org/10.1093/abbs/gmt088> PMID: 23942572
39. Liao X, Xie H, Li S, Ye H, Li S, Ren K, et al. 2', 5'-Oligoadenylate synthetase 2 (OAS2) inhibits zika virus replication through activation of type I interferon signaling pathway. *Viruses*. 2020;12(4):418. <https://doi.org/10.3390/v12040418> PMID: 32276512
40. DeDiego ML, Martínez-Sobrido L, Topham DJ. Novel functions of ifi44l as a feedback regulator of host antiviral responses. *J Virol*. 2019;93(21):e01159-19. <https://doi.org/10.1128/JVI.01159-19> PMID: 31434731
41. Vitour D, Meurs EF. Regulation of interferon production by RIG-I and LGP2: a lesson in self-control. *Sci STKE*. 2007;2007(384):pe20. <https://doi.org/10.1126/stke.3842007pe20> PMID: 17473309

42. Scott MA, Woolums AR, Swiderski CE, Thompson AC, Perkins AD, Nanduri B, et al. Use of nCounter mRNA profiling to identify at-arrival gene expression patterns for predicting bovine respiratory disease in beef cattle. *BMC Vet Res.* 2022;18(1):77. <https://doi.org/10.1186/s12917-022-03178-8> PMID: 35197051
43. Betancor G. You shall not pass: MX2 proteins are versatile viral inhibitors. *Vaccines (Basel).* 2023;11(5):930. <https://doi.org/10.3390/vac-cines11050930> PMID: 37243034
44. de Jong LC, Crnko S, Ten Broeke T, Bovenschen N. Noncytotoxic functions of killer cell granzymes in viral infections. *PLoS Pathog.* 2021;17(9):e1009818. <https://doi.org/10.1371/journal.ppat.1009818> PMID: 34529743
45. Cesar A. Identification of genes associated with intramuscular fat deposition and composition in Nelore breed. Universidade de São Paulo; 2014.
46. Liu B-Q, Liu R-B, Li W-P, Mao X-T, Li Y-N, Huang T, et al. XAF1 prevents hyperproduction of type I interferon upon viral infection by targeting IRF7. *EMBO Rep.* 2023;24(1):e55387. <https://doi.org/10.15252/embr.202255387> PMID: 36394357
47. Sweett H. Genetic mechanisms of male and female cattle fertility. University of Guelph; 2022.
48. Villamayor L, Rivero V, López-García D, Topham DJ, Martínez-Sobrido L, Nogales A, et al. Interferon alpha inducible protein 6 is a negative regulator of innate immune responses by modulating RIG-I activation. *Frontiers in Immunology.* 2023;14.
49. Sánchez JM, Mathew DJ, Behura SK, Passaro C, Charpigny G, Butler ST, et al. Bovine endometrium responds differentially to age-matched short and long conceptuses†. *Biol Reprod.* 2019;101(1):26–39. <https://doi.org/10.1093/biolre/iox060> PMID: 30977805
50. Villamayor L, López-García D, Rivero V, Martínez-Sobrido L, Nogales A, DeDiego ML. The IFN-stimulated gene IFI27 counteracts innate immune responses after viral infections by interfering with RIG-I signaling. *Front Microbiol.* 2023;14:1176177. <https://doi.org/10.3389/fmicb.2023.1176177> PMID: 37187533
51. Larcombe SD, Capewell P, Jensen K, Weir W, Kinnaird J, Glass EJ, et al. Susceptibility to disease (tropical theileriosis) is associated with differential expression of host genes that possess motifs recognised by a pathogen DNA binding protein. *PLoS One.* 2022;17(1):e0262051. <https://doi.org/10.1371/journal.pone.0262051> PMID: 35061738
52. Verhelst J, Hulpiau P, Saelens X. Mx proteins: antiviral gatekeepers that restrain the uninvited. *Microbiol Mol Biol Rev.* 2013;77(4):551–66. <https://doi.org/10.1128/MMBR.00024-13> PMID: 24296571
53. García-Ortega MB, Lopez GJ, Jimenez G, Garcia-Garcia JA, Conde V, Boulaiz H, et al. Clinical and therapeutic potential of protein kinase PKR in cancer and metabolism. *Expert Rev Mol Med.* 2017;19:e9. <https://doi.org/10.1017/erm.2017.11> PMID: 28724458
54. Ramana CV. Regulation of a metabolic gene signature in response to respiratory viruses and type I interferon signaling. *JMP.* 2024;5(1):133–52. <https://doi.org/10.3390/jmp5010009>
55. Morales DJ, Lenschow DJ. The antiviral activities of ISG15. *J Mol Biol.* 2013;425(24):4995–5008. <https://doi.org/10.1016/j.jmb.2013.09.041> PMID: 24095857
56. Fensterl V, Sen GC. Interferon-induced Ifit proteins: their role in viral pathogenesis. *J Virol.* 2015;89(5):2462–8. <https://doi.org/10.1128/JVI.02744-14> PMID: 25428874
57. Jang J-S, Lee J-H, Jung N-C, Choi S-Y, Park S-Y, Yoo J-Y, et al. Rsad2 is necessary for mouse dendritic cell maturation via the IRF7-mediated signaling pathway. *Cell Death Dis.* 2018;9(8):823. <https://doi.org/10.1038/s41419-018-0889-y> PMID: 30068989
58. Tang Z, Mao Y, Ruan P, Li J, Qiu X, Meng Y, et al. Drugs targeting CMPK2 inhibit pyroptosis to alleviate severe pneumonia caused by multiple respiratory viruses. *J Med Virol.* 2024;96(5):e29643. <https://doi.org/10.1002/jmv.29643> PMID: 38695269
59. Feng C, Tang Y, Liu X, Zhou Z. CMPK2 of triploid crucian carp is involved in immune defense against bacterial infection. *Dev Comp Immunol.* 2021;116:103924. <https://doi.org/10.1016/j.dci.2020.103924> PMID: 33186560
60. Talker SC, Barut GT, Lischer HEL, Rufener R, von Münchow L, Bruggmann R, et al. Monocyte biology conserved across species: Functional insights from cattle. *Front Immunol.* 2022;13:889175. <https://doi.org/10.3389/fimmu.2022.889175> PMID: 35967310
61. Hu Y, Wang J, Yang B, Zheng N, Qin M, Ji Y, et al. Guanylate binding protein 4 negatively regulates virus-induced type I IFN and antiviral response by targeting IFN regulatory factor 7. *J Immunol.* 2011;187(12):6456–62. <https://doi.org/10.4049/jimmunol.1003691> PMID: 22095711
62. Zhao P, Jiang T, Zhong Z, Zhao L, Yang S, Xia X. Inhibition of rabies virus replication by interferon-stimulated gene 15 and its activating enzyme UBA7. *Infection, Genetics and Evolution.* 2017;56:44–53.
63. Boys IN, Xu E, Mar KB, De La Cruz-Rivera PC, Eitson JL, Moon B, et al. RTP4 is a potent ifn-inducible anti-flavivirus effector engaged in a host-virus arms race in bats and other mammals. *Cell Host Microbe.* 2020;28(5):712–723.e9. <https://doi.org/10.1016/j.chom.2020.09.014> PMID: 33113352
64. Johnston D, Earley B, McCabe MS, Lemon K, Duffy C, McMenamy M, et al. Experimental challenge with bovine respiratory syncytial virus in dairy calves: bronchial lymph node transcriptome response. *Sci Rep.* 2019;9(1):14736. <https://doi.org/10.1038/s41598-019-51094-z> PMID: 31611566
65. Liew C-C, Ma J, Tang H-C, Zheng R, Dempsey AA. The peripheral blood transcriptome dynamically reflects system wide biology: a potential diagnostic tool. *J Lab Clin Med.* 2006;147(3):126–32. <https://doi.org/10.1016/j.lab.2005.10.005> PMID: 16503242
66. Pinho SS, Alves I, Gaifem J, Rabinovich GA. Immune regulatory networks coordinated by glycans and glycan-binding proteins in autoimmunity and infection. *Cell Mol Immunol.* 2023;20(10):1101–13. <https://doi.org/10.1038/s41423-023-01074-1> PMID: 37582971
67. Pandey VK, Sharma R, Prajapati GK, Mohanta TK, Mishra AK. N-glycosylation, a leading role in viral infection and immunity development. *Mol Biol Rep.* 2022;49(8):8109–20. <https://doi.org/10.1007/s11033-022-07359-4> PMID: 35364718

68. Satyesh CR. Cytokine, cytokine storm and their role in fatalities of COVID-19. *J Infect Dis Immun*. 2021;13(2):20–9. <https://doi.org/10.5897/jidi2021.0216>
69. Righi C, Franzoni G, Feliziani F, Jones C, Petrini S. The Cell-Mediated Immune Response against Bovine alphaherpesvirus 1 (BoHV-1) Infection and Vaccination. *Vaccines (Basel)*. 2023;11(4):785. <https://doi.org/10.3390/vaccines11040785> PMID: 37112697
70. Alcami A. Viral mimicry of cytokines, chemokines and their receptors. *Nat Rev Immunol*. 2003;3(1):36–50. <https://doi.org/10.1038/nri980> PMID: 12511874
71. Benko M, Lenhartová S, Kempová V, Betáková T, Kúdelová M. Chemokine-binding proteins encoded by herpesviruses. *Acta Virol*. 2020;64(2):233–44. https://doi.org/10.4149/av_2020_213 PMID: 32551791
72. Keil GM, Engelhardt T, Karger A, Enz M. Bovine herpesvirus 1 U(s) open reading frame 4 encodes a glycoprotein. *J Virol*. 1996;70(5):3032–8. <https://doi.org/10.1128/JVI.70.5.3032-3038.1996> PMID: 8627780
73. Bryant NA, Davis-Poynter N, Vanderplasschen A, Alcami A. Glycoprotein G isoforms from some alphaherpesviruses function as broad-spectrum chemokine binding proteins. *The EMBO Journal*. 2003;22(4):833–46.
74. Krem MM, Di Cera E. Molecular markers of serine protease evolution. *EMBO J*. 2001;20(12):3036–45. <https://doi.org/10.1093/emboj/20.12.3036> PMID: 11406580
75. Scott MA, Woolums AR, Swiderski CE, Perkins AD, Nanduri B, Smith DR, et al. Whole blood transcriptomic analysis of beef cattle at arrival identifies potential predictive molecules and mechanisms that indicate animals that naturally resist bovine respiratory disease. *PLoS One*. 2020;15(1):e0227507. <https://doi.org/10.1371/journal.pone.0227507> PMID: 31929561
76. Jimenez J, Timsit E, Orsel K, van der Meer F, Guan L, Plastow G. Whole-blood transcriptome analysis of feedlot cattle with and without bovine respiratory disease. *Frontiers in Genetics*. 2021;12(257):257.
77. Witt H, Sahin-Tóth M, Landt O, Chen J-M, Kähne T, Drenth JP, et al. A degradation-sensitive anionic trypsinogen (PRSS2) variant protects against chronic pancreatitis. *Nat Genet*. 2006;38(6):668–73. <https://doi.org/10.1038/ng1797> PMID: 16699518
78. Wang W, Wu L, Wu X, Li K, Li T, Xu B, et al. Combined analysis of serum SAP and PRSS2 for the differential diagnosis of CD and UC. *Clin Chim Acta*. 2021;514:8–14. <https://doi.org/10.1016/j.cca.2020.12.014> PMID: 33333044
79. Sui L, Wang S, Ganguly D, El Rayes TP, Askeland C, Børretzen A, et al. PRSS2 remodels the tumor microenvironment via repression of Tsp1 to stimulate tumor growth and progression. *Nat Commun*. 2022;13(1):7959. <https://doi.org/10.1038/s41467-022-35649-9> PMID: 36575174
80. Lu H, Zhao Z, Yu H, Iqbal A, Jiang P. The serine protease 2 gene regulates lipid metabolism through the LEP/ampk1/SREBP1 pathway in bovine mammary epithelial cells. *Biochem Biophys Res Commun*. 2024;698:149558. <https://doi.org/10.1016/j.bbrc.2024.149558> PMID: 38271832
81. Jones C. Bovine herpes virus 1 (BHV-1) and herpes simplex virus type 1 (HSV-1) promote survival of latently infected sensory neurons, in part by inhibiting apoptosis. *J Cell Death*. 2013;6:1–16. <https://doi.org/10.4137/JCD.S10803> PMID: 25278776
82. Jones C. Herpes simplex virus type 1 and bovine herpesvirus 1 latency. *Clin Microbiol Rev*. 2003;16(1):79–95. <https://doi.org/10.1128/CMR.16.1.79-95.2003> PMID: 12525426
83. Kawai T, Akira S. Innate immune recognition of viral infection. *Nat Immunol*. 2006;7(2):131–7. <https://doi.org/10.1038/ni1303> PMID: 16424890
84. Ackermann MR, Derscheid R, Roth JA. Innate immunology of bovine respiratory disease. *Vet Clin North Am Food Anim Pract*. 2010;26(2):215–28. <https://doi.org/10.1016/j.cvfa.2010.03.001> PMID: 20619180
85. Kim Y, Shin J-S, Nahm M. NOD-like receptors in infection, immunity, and diseases. *Yonsei Med J*. 2016;57(1):5–14.
86. Onomoto K, Onoguchi K, Yoneyama M. Regulation of RIG-I-like receptor-mediated signaling: interaction between host and viral factors. *Cell Mol Immunol*. 2021;18(3):539–55. <https://doi.org/10.1038/s41423-020-00602-7> PMID: 33462384
87. Song J, Li M, Li C, Liu K, Zhu Y, Zhang H. Friend or foe: RIG-I like receptors and diseases. *Autoimmun Rev*. 2022;21(10):103161. <https://doi.org/10.1016/j.autrev.2022.103161> PMID: 35926770
88. Geddes K, Magalhães JG, Girardin SE. Unleashing the therapeutic potential of NOD-like receptors. *Nat Rev Drug Discov*. 2009;8(6):465–79. <https://doi.org/10.1038/nrd2783> PMID: 19483708
89. Yeh Y-J, Tseng C-P, Hsu S-D, Huang H-Y, Lai MMC, Huang H-D, et al. Dual effects of let-7b in the early stage of hepatitis c virus infection. *J Virol*. 2021;95(4):e01800-20. <https://doi.org/10.1128/JVI.01800-20> PMID: 33208444
90. Rosendahl A, Bergmann S, Hammerschmidt S, Goldmann O, Medina E. Lung dendritic cells facilitate extrapulmonary bacterial dissemination during pneumococcal pneumonia. *Front Cell Infect Microbiol*. 2013;3:21. <https://doi.org/10.3389/fcimb.2013.00021> PMID: 23802100
91. Johnston D, Earley B, Cormican P, Murray G, Kenny DA, Waters SM, et al. Illumina MiSeq 16S amplicon sequence analysis of bovine respiratory disease associated bacteria in lung and mediastinal lymph node tissue. *BMC Vet Res*. 2017;13(1):118. <https://doi.org/10.1186/s12917-017-1035-2> PMID: 28464950
92. Cheng Z, Buggiotti L, Salavati M, Marchitelli C, Palma-Vera S, Wylie A, et al. Global transcriptomic profiles of circulating leucocytes in early lactation cows with clinical or subclinical mastitis. *Mol Biol Rep*. 2021;48(5):4611–23. <https://doi.org/10.1007/s11033-021-06494-8> PMID: 34146201
93. Jury EC, Kabouridis PS. New role for Agrin in T cells and its potential importance in immune system regulation. *Arthritis Res Ther*. 2010;12(2):205. <https://doi.org/10.1186/ar2957> PMID: 20398335

94. Iwasaki A, Medzhitov R. Toll-like receptor control of the adaptive immune responses. *Nat Immunol.* 2004;5(10):987–95. <https://doi.org/10.1038/ni1112> PMID: [15454922](https://pubmed.ncbi.nlm.nih.gov/15454922/)
95. Bystrom J, Al-Adhoubi N, Al-Bogami M, Jawad AS, Mageed RA. Th17 lymphocytes in respiratory syncytial virus infection. *Viruses.* 2013;5(3):777–91.
96. McGill JL, Rusk RA, Guerra-Maupome M, Briggs RE, Sacco RE. Bovine gamma delta t cells contribute to exacerbated il-17 production in response to co-infection with bovine rsv and mannheimia haemolytica. *PLoS One.* 2016;11(3):e0151083. <https://doi.org/10.1371/journal.pone.0151083> PMID: [26942409](https://pubmed.ncbi.nlm.nih.gov/26942409/)
97. Veldhoen M. Interleukin 17 is a chief orchestrator of immunity. *Nat Immunol.* 2017;18(6):612–21. <https://doi.org/10.1038/ni.3742> PMID: [28518156](https://pubmed.ncbi.nlm.nih.gov/28518156/)
98. Ma W-T, Yao X-T, Peng Q, Chen D-K. The protective and pathogenic roles of IL-17 in viral infections: friend or foe?. *Open Biol.* 2019;9(7):190109. <https://doi.org/10.1098/rsob.190109>
99. Mills KHG. IL-17 and IL-17-producing cells in protection versus pathology. *Nat Rev Immunol.* 2023;23(1):38–54. <https://doi.org/10.1038/s41577-022-00746-9> PMID: [35790881](https://pubmed.ncbi.nlm.nih.gov/35790881/)
100. Schwarz D, Lipoldová M, Reinecke H, Sohrabi Y. Targeting inflammation with collagen. *Clin Transl Med.* 2022;12(5):e831. <https://doi.org/10.1002/ctm2.831> PMID: [35604877](https://pubmed.ncbi.nlm.nih.gov/35604877/)
101. Tomlin H, Piccinini AM. A complex interplay between the extracellular matrix and the innate immune response to microbial pathogens. *Immunology.* 2018;155(2):186–201. <https://doi.org/10.1111/imm.12972> PMID: [29908065](https://pubmed.ncbi.nlm.nih.gov/29908065/)
102. Balboa MA, Balsinde J. Phospholipases: from structure to biological function. *Biomolecules.* 2021;11(3).
103. Pungertar J, Bihl F, Lambeau G, Križaj I. What do secreted phospholipases A2 have to offer in combat against different viruses up to SARS-CoV-2?. *Biochimie.* 2021;189:40–50. <https://doi.org/10.1016/j.biochi.2021.05.017> PMID: [34097986](https://pubmed.ncbi.nlm.nih.gov/34097986/)
104. Paul A, Tang TH, Ng SK. Interferon Regulatory factor 9 structure and regulation. *Front Immunol.* 2018;9.
105. Bravo Garcia-Morato M, Calvo Apalategi A, Bravo-Gallego LY, Blázquez Moreno A, Simón-Fuentes M, Garmendia JV, et al. Impaired control of multiple viral infections in a family with complete IRF9 deficiency. *J Allergy Clin Immunol.* 2019;144(1):309-312.e10. <https://doi.org/10.1016/j.jaci.2019.02.019> PMID: [30826365](https://pubmed.ncbi.nlm.nih.gov/30826365/)